Locking A Three-Mirror Optical Cavity : A Negative Imaginary Systems Approach

Mohamed A. Mabrok, Abhijit G. Kallapur, Ian R. Petersen,
Dirk Schütte, Toby K. Boyson, and Alexander Lanzon

***Abstract*— In this paper, we present an example of control system design based on negative imaginary (NI) system theory. The system under consideration is an optical cavity system. A dynamical model of the cavity system is obtained through system identification of applied to experimental input output frequency response data obtained using a digital signal analyzer (DSA). The identified model satisfies NI property. An integral resonant controller is designed based on the NI system theory.**

***Index Terms*— Negative imaginary systems, optical cavity, integral resonant control.**

I. Introduction

In many modern physics experiments, the use of an optical cavity has become an important tool for enhancement in detection sensitivity [1]–[3], nonlinear interactions, and quantum dynamics [4]. An important application of optical cavities is in laser physics itself. However, there are many applications of external optical cavities (independent from lasers) that take advantage of the common physical properties associated with resonator physics. For example, cavity locking arises in the frequency stabilization of semiconductor lasers [5], cavity-enhanced spectroscopic techniques [1]–[3], cavity quantum electrodynamics [6], microcavities [7], [8], as well as in general atomic, molecular, and optical physics [4]. Indeed, the characteristic of the optical cavity allow physicists to study the interaction between matter and the applied field [9]. Also, a cavity allows one to impose a well-defined mode structure on the electromagnetic field [10] and to study manifestly quantum mechanical behavior associated with the modified vacuum structure and/or the large field associated with a single photon confined to a small volume [4].

The structure of optical cavities involves an arrangement of mirrors that forms a standing wave in the cavity resonator. The light source is usually a continuous or discrete laser source. To form the standing wave inside the cavity, the resonant frequency of the cavity must match the input laser frequency. In this case, the cavity is said to be in *lock* with the input laser frequency.

Feedback control plays an important role in cavity locking. For example, in [11]–[14], feedback control is used to stabilize an optical cavity in order to build maximum energy inside these cavities. The meaning of stability here, is to keep the cavity in lock with the frequency of the input laser.

The difference between the resonant frequency of the cavity and the input laser frequency is characterized in terms of a *detuning parameter* Δ. The control goal is to keep this detuning parameter $\Delta = 0$. Since the cavity resonant frequency is directly dependent on the distance between the cavity mirrors, it is possible to force the detuning parameter Δ to zero by varying the distance between these mirrors. The use of piezo-electic transducer (PZT) material can play an important role in moving the cavity mirrors to achieve the required resonant frequency. The control methodology here is to measure the detuning parameter Δ, then using this measured Δ for feedback through a controller to generate voltage applied to a PZT actuator attached to one of the cavity mirrors; see Fig. 1.

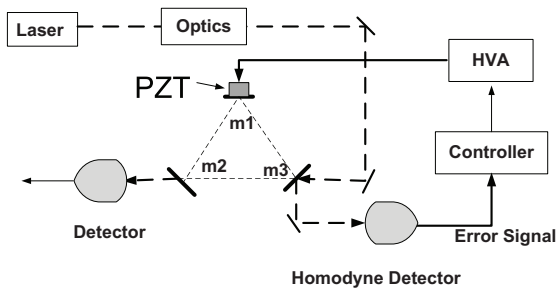

Fig. 1. Locking scheme for a three-mirror ring cavity: The optical signals are represented by dash-dot lines and the electrical signals are represented as solid lines.

The representation of a cavity system in Fig. 1 involves a collocated force actuator (the PZT actuator) combined with a position sensor (the cavity itself). This implies that the cavity system under consideration can be considered using the recently developed theory called negative imaginary systems theory [15]–[18].

Negative imaginary (NI) systems were introduced by Lanzon and Petersen in [15]. Such systems are defined so that the imaginary part of the transfer function $G(s) = D + C(sI - A)^{-1}B$, satisfies the condition $j\left(G(j\omega) - G(j\omega)^*\right) \geq 0$ for all $\omega \in (0, \infty)$. Xiong et. al. extended NI systems theory

This work was supported by the Australian Research Council.

Mohamed Mabrok, Abhijit Kallapur, Toby K. Boyson and Ian Petersen are with the School of Engineering and Information Technology, University of New South Wales at the Australian Defence Force Academy, Canberra ACT 2600, Australia, email:abdallamath@gmail.com, abhijit.kallapur@gmail.com, i.r.petersen@gmail.com, tkboyson@gmail.com

Alexander Lanzon is with the Control Systems Centre, School of Electrical and Electronic Engineering, University of Manchester, Manchester M13 9PL, United Kingdom, email:Alexander.Lanzon@manchester.ac.uk

D. Schütte is with the Centre for Quantum Engineering and Space-Time Research, Leibniz Universität, Hannover 30167, Germany. dirk.schuette@aei.mpg.de.

 © 2012 Engineers Australia

in [17] by allowing for simple poles on the imaginary axis of the complex plane except at the origin. Furthermore, NI controller synthesis has also been discussed in [15]. In addition, it has been shown in [15] that a necessary and sufficient condition for the internal stability of a positive-feedback interconnection of an NI system with transfer function matrix $G(s)$ and an strictly negative imaginary (SNI) system with transfer function matrix $C(s)$ is given by the DC gain condition $\lambda_{max}(G(0)C(0)) < 1$. Here, the notation $\lambda_{max}(\cdot)$ denotes the maximum eigenvalue of a matrix with only real eigenvalues. Also, a further extension of the stability results is presented in [18].

Many practical systems can be considered as NI systems. For example, such systems arise when considering the transfer function from a force actuator to a corresponding collocated position sensor (for instance, a piezoelectric sensor) in a lightly damped structure [16], [19]–[21]. Also, stability results for interconnected systems with an NI frequency response have been applied to the decentralized control of large vehicle platoons in [22]. In [22], the authors discuss the stability of various designs to enhance the robust stability of the system with respect to small variations in coupling gains.

In this paper, we apply the stability results presented in [15], [17] to design a controller for the cavity system shown in Fig. 1. Experimental frequency response data for the cavity system is recorded using a digital signal analyzer and a state space model is obtained using the *System Identification Toolbox* from Matlab®. Then, an integral resonant controller is designed to damp the PZT resonance.

According to the results in [15], [17], the positive-feedback interconnection of an NI system and an SNI system is internally stable if and only if the DC gain is less than one. The identified model for the cavity satisfies the NI property.

Unlike the control techniques applied to experimental quantum optics presented in [11]–[14], where the linear quadratic Gaussian (LQG) controller synthesis was discussed, the proposed NI technique guarantees the robustness of the closed-loop with respect to changes in the plant resonant frequencies.

The rest of the paper is organized as follows: Section II discusses the structure of the three-mirror ring cavity. Section III describes the process of obtaining a state space model for the cavity system, starting with the experimental frequency response data and shows that the system model is NI. The design of an integral resonant controller for the cavity system is discussed in Section IV. The paper is concluded with final remarks in Section V.

II. Cavity System

The cavity system under consideration is a three-mirror open-air ring cavity as shown in Fig. 1, a PZT is mounted on mirror m1 which is used to vary the length of the cavity hence the resonant frequency of the cavity. The laser source in this experiment is continuous-wave 1550 nm diode laser. Before coupling the light into the cavity, it is modified using optics such as isolators, mode matching optics, half wave plates, and beam splitters. Then the light is propagated to the mirror m3. There are two outputs of this cavity, the first output is the transmitted beam, which is detected at the transmitted port by a photodetector at the output of mirror m2. This output is not used for cavity locking. The second output is the error signal which is detected at mirror m3 using homodyne detection; see e.g., [13], [14]. This error signal, detected using a homodyne detection, is fed to the integral resonant controller and then to a high voltage amplifier (HVA) before providing the necessary control signal to the PZT actuator.

The control objective is to drive the error signal to zero so as to achieve cavity locking ($\Delta \approx 0$) while maintaining the transmitted signal at a maximum. This ensures that the cavity operates in a linear region as depicted in the calculated plot for the error signal in Fig. 2.

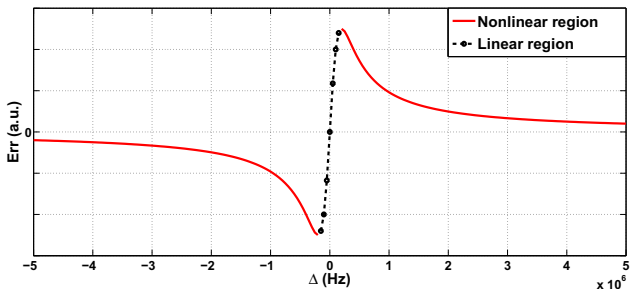

Fig. 2. Calculated variation of the error signal (output of homodyne detector) with the detuning parameter Δ.

III. Cavity Model and System Identification

To obtain a dynamic model for the cavity system, a system identification method is used to determine a state-space model from the experimental input output frequency response data. We record the frequency response of the cavity system using a digital signal analyzer as shown in Fig. 3. The cavity was held in lock using a manually tuned analog PI controller when the frequency response data was collected as shown in Fig. 3.

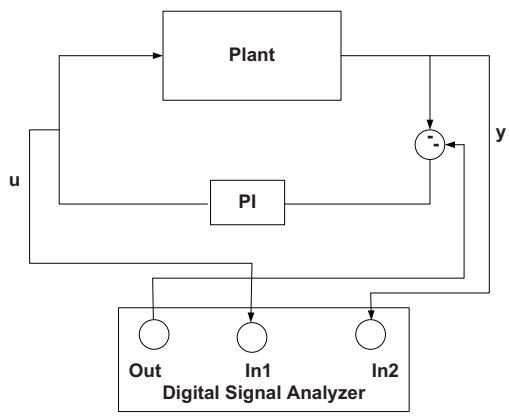

Fig. 3. Block diagram of the the digital signal analyzer setup used to obtain the frequency response data for the plant.

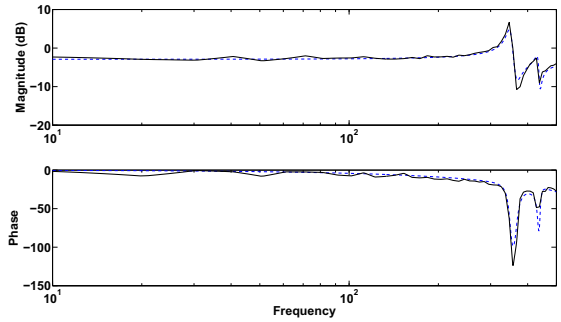

Fig. 4. The solid line is the frequency response data for the plant obtained from the DSA, and the dashed line is the identified model.

The identified state space model of the cavity system is given as following;

$$\dot{x}(t) = Ax(t) + Bu(t), \tag{1}$$
$$y(t) = Cx(t) + Du(t). \tag{2}$$

This model can be written as a sum of a second order systems as following;

$$G(s) = \sum_{i=1}^{3} \frac{k_i}{s^2 + 2\zeta\omega_i + \omega_i^2}, \tag{3}$$

where the parameters ζ_i, ω_i and k_i are given in the Table I.

i	1	2	3
ζ_i	25×10^{-3}	40.2×10^{-3}	99.2×10^{-2}
ω_i	22×10^2	26.3×10^2	51×10^2
k_i	3×10^5	11×10^4	14×10^6

TABLE I
MODEL PARAMETERS

The state space model (1)-(2) is satisfies the NI property. This can be verified from the Bode plot of the model in Fig. 5, since the phase lies between 0 and $-\pi$ for all $\omega > 0$, see [16].

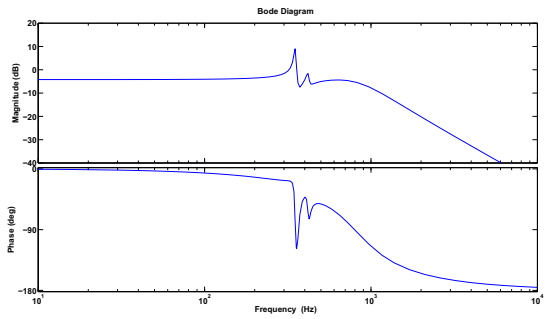

Fig. 5. Bode plot of identified cavity model which shows that the phase lies between 0 and $-\pi$ for all $\omega > 0$.

Also, the imaginary part of the model transfer function is plotted in Fig.6, which shows that it is negative over the bandwidth of interest.

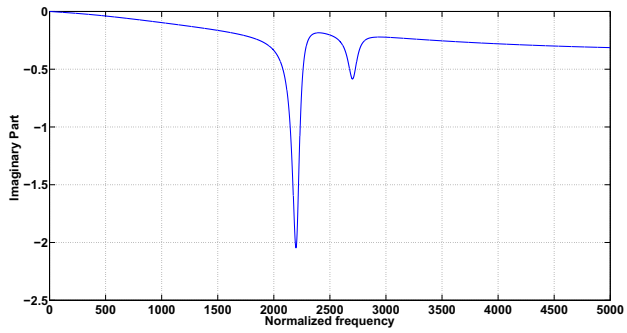

Fig. 6. The imaginary part of the model transfer function, which shows that it is negative over the bandwidth of interest.

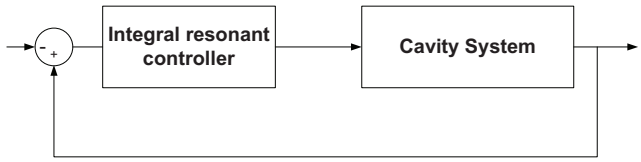

Fig. 7. Integral resonant controller with the cavity model.

IV. CONTROLLER DESIGN

In this paper, an integral resonant controller [16], [23] with a feed-through is used, which has a transfer function as follows:

$$C(s) = \frac{\Gamma}{s + \Phi\Gamma} - D. \tag{4}$$

The controller in (4) is SNI for any $\Gamma > 0$ and $\Phi > 0$.

The proposed integral resonant control scheme is shown diagrammatically in Fig. 7. According to the stability results in [15], [17], [18], the closed loop system for the cavity system and the integral resonant controller in (4) is internally stable providing the DC gain condition $\lambda_{max}(C(0)G(0)) < 1$ is satisfied.

The DC gain condition $\lambda_{max}(C(0)G(0)) < 1$ can be guaranteed with the feed-through gain D. Also, the large D is used to reduce the steady state error. The controller (4) can be considered as a lead compensator since it have one pole and one zero in the left half of the complex plane.

The integral resonant controller design process that we used can be summarized as following:

- Determine the DC gain that required to give the desired steady state error, where $erorr = \frac{1}{1-G(0)C(0)}$ and $C(0) = \frac{1}{\Phi} - D$.
- Using Nyquist plot to determine the phase margin of the loop gain $-C(0)G(s)$.
- Choose the location of the zero and the pole of the controller such that the phase margin is greater that 30° and the maximum phase lead of the controller occurs at the gain crossover frequency.

In our case, we chose the steady state error to be less than 0.06 and to achieve that, a DC gain for the controller is chosen to be $C(0) = -30$ dB. The resulting phase margin

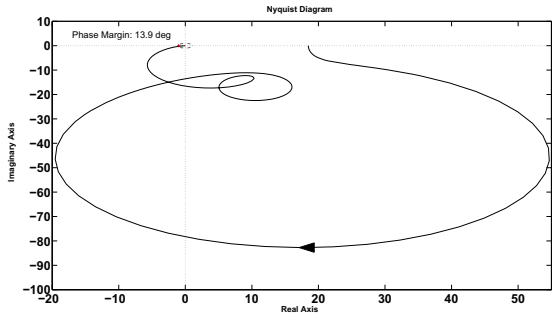

Fig. 8. Nyquist plot of $-C(0)G(s)$ which shows that the phase margin is $14°$.

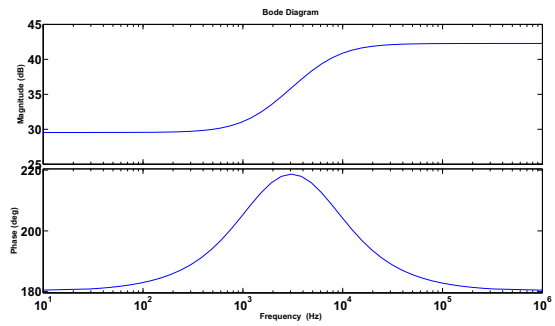

Fig. 9. Bode plot of the integral resonant controller with a transfer function $C(s) = \frac{\Gamma}{s+\Phi\Gamma} - D$, where $\Phi = 0.01, D = 130$ and $\Gamma = 40 \times 10^5$.

of the loop-gain $-C(0)G(s)$ is $14°$ as shown in the Nyqust plot given in Fig. 8.

Then, the controller parameters were chosen such that the controller has a maximum phase shift $35°$ as shown Bode plot given in Fig. 9.

Finally, to verify the performance of the closed loop system, the step response and Bode plot of the closed loop are plotted in Fig. 10 and Fig. 11 respectively.

V. Conclusion

In this paper, a dynamical model of a cavity system is obtained through system identification applied to experimental

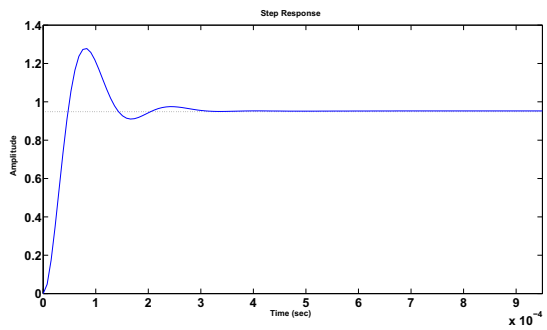

Fig. 10. The step response of the closed-loop system corresponding to an integral resonant controller with a transfer function $C(s) = \frac{\Gamma}{s+\Phi\Gamma} - D$, where $\Phi = 0.01, D = 130$ and $\Gamma = 40 \times 10^5$.

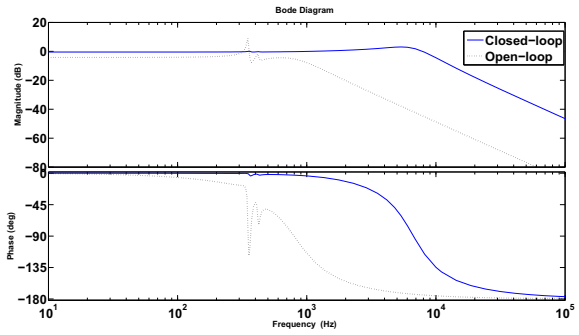

Fig. 11. Open- and closed-loop frequency responses for the cavity system and an integral resonant controller with a transfer function $C(s) = \frac{\Gamma}{s+\Phi\Gamma} - D$, where $\Phi = 0.01, D = 130$ and $\Gamma = 40 \times 10^5$. These parameters are chosen to provide adequate damping of the resonant mode.

input output frequency response data. The data was recorded using a digital signal analyzer. The system model is shown to be negative imaginary (NI) system. An integral resonant controller is designed based on the NI system theory. Simulation results for the closed-loop have been provided. Future research will be directed towards implementing this controller experimentally.

References

[1] B. A. Paldus, C. C. Harb, T. G. Spence, B. Wilke, J. Xie, J. S. Harris, and R. N. Zare, "Cavity-Locked Ring-Down Spectroscopy," *Journal of Applied Physics*, vol. 83, no. 8, pp. 3991–3997, Apr. 1998.

[2] A. G. Kallapur, T. K. Boyson, I. R. Petersen, and C. C. Harb, "Nonlinear estimation of ring-down time for a fabry-perot optical cavity," *Optics Express*, vol. 19, no. 7, pp. 6377–6386, 2011.

[3] ——, "Offline estimation of ring-down time for an experimental fabry-perot optical cavity," in *IEEE International Conference on Control Applications (CCA)*, Denver, CO, USA, September 2011, pp. 556–560.

[4] J. Ye and T. W. Lynn, "Applications of optical cavities in modern atomic, molecular, and optical physics," ser. Advances In Atomic, Molecular, and Optical Physics. Academic Press, 2003, vol. 49, pp. 1–83.

[5] L. H. B. Dahmani and R. Drullinger, "Frequency stabilization of semiconductor lasers by resonant optical feedback," *Optics Letters*, vol. 12, no. 11, pp. 876–878, 1987.

[6] H. Mabuchi and A. C. Doherty, "Cavity quantum electrodynamics: Coherence in context," *Science*, vol. 298, no. 5597, pp. 1372–1377, 2002.

[7] K. J. Vahala, "Optical microcavities," *Nature*, vol. 424, pp. 839–846, 2003.

[8] F. V. Jan Klaers, Julian Schmitt and M. Weitz, "Bose-Einstein Condensation of Photons in an Optical Microcavity," *Nature*, vol. 468, pp. 545–548, 2010.

[9] J. P. Reithmaier, G. Sek, A. Loffler, C. Hofmann, S. Kuhn, S. Reitzenstein, L. V. Keldysh, V. D. Kulakovskii, T. L. Reinecke, and A. Forchel, "Strong coupling in a single quantum dot-semiconductor microcavity system," *Nature*, vol. 432, no. 7014, pp. 197–200, Nov. 2004. [Online]. Available: http://dx.doi.org/10.1038/nature02969

[10] D. Dragoman and M. Dragoman, *Quantum-Classical Analogies*. Springer, 2004.

[11] E. H. Huntington, M. R. James, and I. R. Petersen, "Modern quantum control applied to optical cavity locking," in *Australian Institute of Physics 17th National Congress 2006*, Brisbane, QLD, December 2006.

[12] ——, "Laser-cavity frequency locking using modern control," in *46th IEEE Conference on Decision and Control*, New Orleans, LA, USA, December 2007, pp. 6346 – 6351.

[13] S. Z. Sayed Hassen, E. H. Huntington, I. R. Petersen, and M. R. James, "Frequency locking of an optical cavity using LQG integral control," in *Proceedings of the 17th IFAC World Congress*, Seoul, Korea, July 2008, pp. 1821–1826.

[14] S. Z. S. Hassen, M. Heurs, E. H. Huntington, I. R. Petersen, and M. R. James, "Frequency locking of an optical cavity using linear quadratic Gaussian integral control," *Journal of Physics B: Atomic, Molecular and Optical Physics*, vol. 42, p. 175501, 2009.

[15] A. Lanzon and I. R. Petersen, "Stability robustness of a feedback interconnection of systems with negative imaginary frequency response," *IEEE Transactions on Automatic Control*, vol. 53, no. 4, pp. 1042–1046, 2008.

[16] I. R. Petersen and A. Lanzon, "Feedback control of negative imaginary systems," *IEEE Control System Magazine*, vol. 30, no. 5, pp. 54–72, 2010.

[17] J. Xiong, I. R. Petersen, and A. Lanzon, "A negative imaginary lemma and the stability of interconnections of linear negative imaginary systems," *IEEE Transactions on Automatic Control*, vol. 55, pp. 2342–2347, 2010.

[18] M. A. Mabrok, A. G. Kallapur, I. R. Petersen, and A. Lanzon, "Stability analysis for a class of negative imaginary feedback systems including an integrator," in *Proc. 8th Asian Control Conf. (ASCC)*, 2011, pp. 1481–1486.

[19] J. L. Fanson and T. K. Caughley, "Positive position feedback control for large space structures," *AIAA Journal*, vol. 28, no. 4, pp. 717–724, Apr. 1990.

[20] B. Bhikkaji and S. Moheimani, "Fast scanning using piezoelectric tube nanopositioners: A negative imaginary approach," in *Proc. IEEE/ASME Int. Conf. Advanced Intelligent Mechatronics AIM 2009*, Singapore, July 2009, pp. 274–279.

[21] Y. K. Yong, B. Ahmed, and S. O. R. Moheimani, "Atomic force microscopy with a 12-electrode piezoelectric tube scanner," *Review of Scientific Instruments*, vol. 81, no. 3, March 2010.

[22] C. Cai and G. Hagen, "Stability analysis for a string of coupled stable subsystems with negative imaginary frequency response," *IEEE Transactions on Automatic Control*, vol. 55, pp. 1958–1963, Aug. 2010.

[23] S. S. Aphale, A. J. Fleming, and S. O. R. Moheimani, "Integral control of smart structures," *Smart Mater. Struct.*, vol. 16, p. 439446, 2007.